

Muscarinic acetylcholine receptor produced in recombinant baculovirus infected *Sf9* insect cells couples with endogenous G-proteins to activate ion channels

Subhash Vasudevan^b, Louis Premkumar^c, Sally Stowe^d, Peter W. Gage^c, Helmut Reiländer^c and Shin-Ho Chung^a

^aProtein Dynamics Unit, Department of Chemistry, ^bResearch School of Chemistry, ^cJohn Curtin School of Medical Research and ^dResearch School of Biological Sciences, Australian National University, Canberra, ACT 2601, Australia and ^eMax Planck Institut für Biophysik, Frankfurt, Germany

Received 13 July 1992; revised version received 31 August 1992

Following the infection of insect ovarian cells (*Sf9*) with recombinant baculovirus bearing the cDNA coding for the rat muscarinic acetylcholine (ACh) receptor subtype m3, ionic flux across the membrane in response to the application of ACh was examined electrophysiologically. We show that ACh activates potassium currents. The response is abolished when cells are treated with pertussis toxin. No ACh-induced currents are observed from uninfected cells or cells infected with virus which do not contain the cDNA coding for ACh receptors in its genome. The characteristics of single channel currents show time-dependent changes following the application of ACh. Initially, ACh activates brief channel currents with a conductance of about 5 pS. The conductance level of channels gradually increases in steps to 10 pS and then to 20 pS and 40 pS. At the same time, channel open probability also increases. Thereafter, additional channels appear, opening and closing independently of, or at times in synchrony with, the original channel.

Muscarinic acetylcholine receptor; Baculovirus expression; Patch clamp; G-protein; Potassium channel

1. INTRODUCTION

Acetylcholine at nicotinic sites rapidly activates ion channels that are permeable to sodium and potassium ions [1]. In contrast, acetylcholine at muscarinic receptors mediates a wide variety of responses, such as inhibition of adenylyl cyclase, stimulation of phosphatidylinositol metabolism and release of calcium from intracellular stores, all of which are relatively slow because the signals are transduced via guanine nucleotide-binding proteins (G-proteins). Five sub-types of muscarinic receptors, m1–m5, have been cloned and sequenced. Based on similarities in the second messenger-mediated responses, m1, m3 and m5 receptors have been classified together, whilst m2 and m4 sub-types form a second group [2]. Electrophysiological studies of cell lines (mouse fibroblast A9-L cells, neuroblastoma-glioma NG108-15 cells and CHO cells) producing discrete muscarinic sub-types have indicated that m1, m3 and m5 receptors activate calcium-dependent potassium conductances, whereas m2 and m4 receptors do not [3–5].

The baculovirus expression system is gaining popularity as a method of choice for producing large levels of proteins for biochemical and biophysical characteri-

sation. The *Shaker* channels [6] and the cystic fibrosis gene product [7], which are known to directly conduct ions, have been produced in *Sf9* cells and examined electrophysiologically. These studies have indicated that the insect cells are highly suited for patch clamping. The method of producing the m3 receptor in the membrane of ovarian cells of the insect, *Spodoptera frugiperda*, using the recombinant baculovirus, has been described previously [8]. Here we demonstrate that the rat m3 muscarinic receptor, which is not known to conduct ions, can, upon stimulation by acetylcholine, couple with endogenous second messengers in the insect cells to modulate ion channels. The results we obtained with the insect cells are consistent with studies on mammalian cells [3–5]. We have extended these earlier studies to analyse channel currents using a newly developed signal processing system [9,10].

2. MATERIALS AND METHODS

2.1. Cells and viruses

The construction of recombinant AcMNPV bearing the M3 cDNA has been described by Vasudevan et al. [8]. The recombinant AcMNPV bearing the *lacZ* gene coding for β -galactosidase [11], which was used as a negative control for our experiments, was obtained from T. Tiganis (St. Vincent's Medical Research Institute, Melbourne, Australia). *Spodoptera frugiperda* cells (*Sf9*) (ATCC accession number CRL 1711) were propagated at 27°C in TNM-FH medium supplemented with 10% fetal calf serum. Gentamycin at 50 μ g ml⁻¹ and pluronic F68 at 0.02% (w/v) were also present in the medium. The

Correspondence address: S.H. Chung, Protein Dynamics Unit, Department of Chemistry, Australian National University, Canberra, ACT 2601, Australia. Fax: (61) (6) 247 2792.

procedures for cell culture and viral infections for protein production were carried out as described by Summers and Smith [13]. Briefly, 2×10^6 Sf9 cells were transferred to a 25 cm² tissue culture flask and allowed to attach for 30 min. Cell culture medium with the supplements was added to a final volume of 5 ml and incubated at 27°C. After 48 h, the cells were infected with the appropriate recombinant virus (multiplicity of infection, MOI = 10). Electrophysiological experiments were performed with infected Sf9 cells and the appropriate controls at time intervals of 24, 48 and 72 h post-infection. For some experiments, pertussis toxin was added to a final concentration of 2 $\mu\text{g ml}^{-1}$ to the cells at the point of infection and cells were harvested at appropriate intervals. All chemicals used were obtained from Sigma.

2.2. Electrical recording

Currents were recorded from whole cells or cell-attached patches with borosilicate glass pipettes that had a resistance of 10–15 M Ω . The composition of the pipette solution in mM was, for whole-cell experiments: KCl 140; MgCl₂ 1; GTP 0.25; ATP 0.4; HEPES-KOH 10 (pH 7.2); and for cell-attached single channel recording: NaCl 140; KCl 5; CaCl₂ 2; MgCl₂ 1; HEPES-NaOH 10 (pH 7.2). The bath was perfused with an oxygenated solution (pH 7.2) containing in mM: NaCl 126; KCl 2.5; MgCl₂ 1; CaCl₂ 2; NaH₂PO₄ 0.12; NaHCO₃ 26; D-glucose, 25.

Whole-cell currents were recorded at a holding potential of -40 mV. Application of acetylcholine activated outward currents which reversed polarity close to the potassium equilibrium potential. Single channel currents activated by addition of acetylcholine to the bath were recorded in cell-attached patches. The potential across a cell-attached patch is equal to the difference between the resting membrane potential of the cell (V_m) and the potential in the pipette (V_p), namely, $V_m - V_p$ measured with respect to the bath potential. For example, if the membrane potential is -60 mV and the pipette potential is also -60 mV then the potential across the membrane under the patch electrode will be 0 mV. As the pipette potential is made more positive the potential across the patch becomes more negative (hyperpolarized). The driving force on potassium ions when a potassium-selective channel in a patch opens would be $V_m - V_p - E_K$ where E_K is the potassium equilibrium potential. If a channel in a patch opens and the current reverses at a pipette potential V_R , then $E_o = V_m - V_R$, where E_o is the potential across the patch at which net ion flux across the channel is zero.

Currents were recorded with a current-to-voltage converter (Axopatch 200, Axon Instruments). The current traces recorded from whole-cell configurations were filtered at 1 kHz and sampled at 2 kHz, while single channel currents were filtered at 2 or 5 kHz and sampled at 5 or 10 kHz. The digitized records were stored on magnetic disks for subsequent analysis. When needed, the single channel currents were analysed using the digital signal processing techniques based on Hidden Markov Models [9,10].

3. RESULTS

3.1. Whole-cell currents

In response to 50 μM acetylcholine all but 2 of the 25 cells infected with recombinant virus bearing the m3 cDNA produced a pronounced outward current when the membrane potential was clamped at -40 mV (Fig. 1Aa). In contrast, no discernible current was observed in any of the 14 cells that were either not infected with virus or were infected with the *lacZ* virus which does not contain the cDNA coding for the m3 muscarinic receptor (Fig. 1Ab and Ac). The acetylcholine-induced response could be observed in the cells that had been infected with the recombinant virus for 24 h ($n = 10$), 48 h ($n = 8$) and 72 h ($n = 5$). Thereafter, it became difficult to form a tight seal between the rim of the electrode and the cell surface as the infected cells began to die.

The transmembrane current induced by acetylcholine in infected cells could be abolished when they were exposed to 2 $\mu\text{g ml}^{-1}$ of pertussis toxin for 48 to 72 h ($n = 5$) (Fig. 1Ad). As shown in Fig. 1B, changing the potential towards hyperpolarized potentials reduced the current amplitude and the current reversed polarity at a membrane potential of around -80 mV, which is close to the reversal potential calculated from the Goldman-Hodgkin-Katz equation with a $P_{\text{Na}}/P_{\text{K}}$ ratio of 0.02.

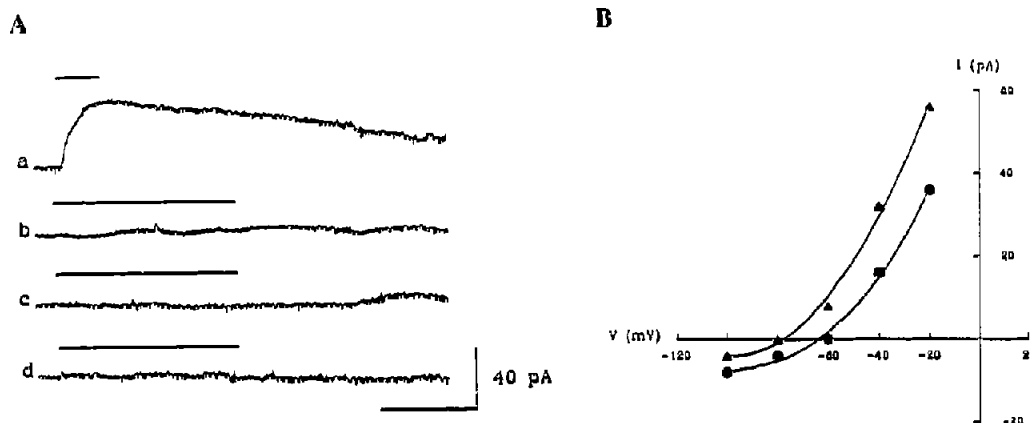


Fig. 1. Transmembrane currents mediated by m3 muscarinic acetylcholine receptors. (A) A pronounced outward current appeared following the bath application of 50 μM acetylcholine when the membrane potential of the cell was clamped at -40 mV (trace a). The current flux could only be observed in the cells which were infected with the recombinant virus bearing the cDNA coding for m3 muscarinic receptor. Records obtained from an uninfected cell (trace b) and a cell infected with the *lacZ* virus (trace c) showed no deflection in the current level when the same concentration of acetylcholine was applied. A cell infected with the recombinant virus and pre-treated with pertussis toxin did not show any response to acetylcholine application (trace d). The duration of bath application of acetylcholine is indicated by the bar above the current records in traces a–d. The horizontal bar represents 200 s for trace a and 50 s for traces b–d. (B) Current-voltage curves for Sf9 cells infected with recombinant virus producing m3 muscarinic receptor. The concentrations of K⁺ in the pipette were 2.5 mM (Δ) and 15 mM (\bullet).

Changing the external potassium concentration from 2.5 to 15 mM shifted the reversal potential from around -80 mV to -55 mV (Fig. 1B), again in agreement with the P_{Na}/P_K ratio of 0.02.

3.2. Cell-attached patches

Single channel currents were recorded from a total of 59 cell-attached patches in response to $50 \mu\text{M}$ acetylcholine applied to the area outside the patch. Following the application of acetylcholine, channel currents were elicited in 20 of 43 cells infected with the recombinant virus, but none of 16 uninfected cells or cells infected with virus which did not bear cDNA coding for the m3 muscarinic receptor. The currents were outward at a pipette potential of -60 mV. When the pipette potential was made less negative, the single channel current amplitude decreased and reversed in direction close to the resting membrane potential. Similar currents were seen when the pipette solution contained sodium gluconate instead of sodium chloride, suggesting that the current is not carried by chloride ions. The channel characteristics were essentially the same when the bath solution was replaced with a solution containing 140 mM KCl and currents were recorded at a pipette potential of 0 mV. In a few cells, inside-out patches were formed at the end of the experiment and no channel activity was observed. These observations confirmed that the channel was predominantly permeable to potassium ions.

The characteristics of single channel currents activated by acetylcholine underwent pronounced time-dependent changes. In Fig. 2a, the sequence of changes following the application of the acetylcholine is illustrated with a compressed time scale. Within 30 s after the application of $50 \mu\text{M}$ acetylcholine, occasional, small amplitude currents were apparent and the frequency of opening and closing steadily increased with time. Because of their small amplitudes relative to the background noise, we used a digital processing technique to characterize these channels. A 1,000-point sample segment of record, representing 100 ms of real time, is shown in Fig. 2b. The standard deviation of the noise, before channel currents were activated, was 0.35 pA when the cut-off frequency of the low pass filter was 5 kHz. Using the signal processing technique, we extracted the harmonic interferences, composed of 50, 150 and 250 Hz, contained in the record, a drift of the baseline approximated as a cubic function of time (not shown here) and the sequence of channel currents (Fig. 2c). The record contained two distinct current amplitudes of 0.32 and 0.64 pA. The corresponding conductances are (if we assume that the membrane potential of the cell was -60 mV) 5.3 and 10.7 pS. The probability of the channel being open at the 0.32 pA level was 0.37, with a mean open duration of 0.8 ms. Openings to the 0.64 pA level, on the other hand, were infrequent, with a probability of 0.09, but the mean open time was 2.3

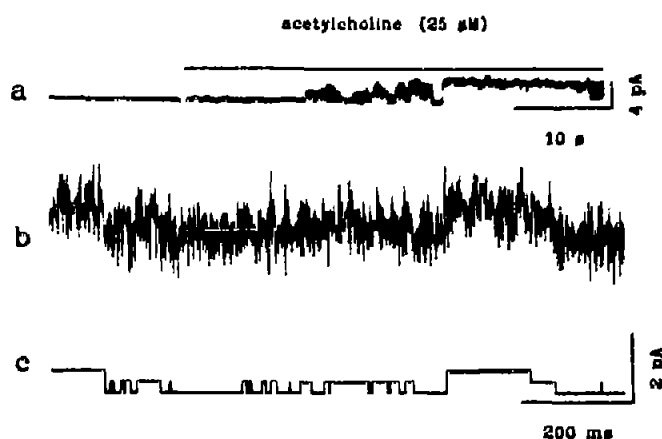


Fig. 2. Appearance of small single channels from a cell-attached patch. The time-dependent changes of the currents recorded just before and following the application of $50 \mu\text{M}$ acetylcholine are shown in trace a. The first segment in trace a is the background noise in the absence of channel currents. Shortly after the application of acetylcholine, channel currents of progressively increasing amplitudes are activated. An example of channel current recorded from a cell-attached patch about 30 s after exposure of the cell to $50 \mu\text{M}$ acetylcholine is shown in trace b in an expanded time scale. The record was filtered at 5 kHz and sampled at 10 kHz. Maximum likelihood estimates of channel currents, baseline drift and A.C. hum were obtained using digital signal processing techniques. The record contained a slow baseline drift and a harmonic wave composed of 50, 150 and 250 Hz (not shown here) and single channel currents of two distinct amplitudes, 0.32 pA and 0.64 pA (trace c).

ms. From the 0.64 pA level, the current level returned either instantaneously to the baseline ($P = 0.018$) or to the 0.32 pA level ($P = 0.024$).

The amplitudes of channel currents thereafter increased progressively with time, reaching at times 7–9 pA. In Fig. 3, sequential amplitude histograms are displayed as a three-dimensional graph. A sample 1,000-point segment taken from each record is displayed in the right hand column. The records used to construct the first three histograms were taken at approximately 1 min intervals, whereas those used to obtain the last two histograms were taken at 5 s interval. The record taken immediately after the addition of acetylcholine to the bath solution showed no channel activity, indicated by a sharp amplitude peak at the baseline (curve labelled a). The next histogram shows, in addition to a skewed baseline distribution, a distinct peak at about 1.2 pA (Fig. 3Ab). The amplitude of this peak increased slightly at first (Fig. 3Ac) and then drastically (Fig. 3Ad) in the following histograms. In the latter amplitude histograms, there appeared a further small peak at 2.3 pA. A short time later, this peak became the most prominent one, the broad spread centred around 2.3–2.7 pA.

The amplitude of channel currents continued to increase with time in increments of approximately 2.5 pA. Most of the time, the channel remained open at one of the sublevels, occasionally returning to the fully closed

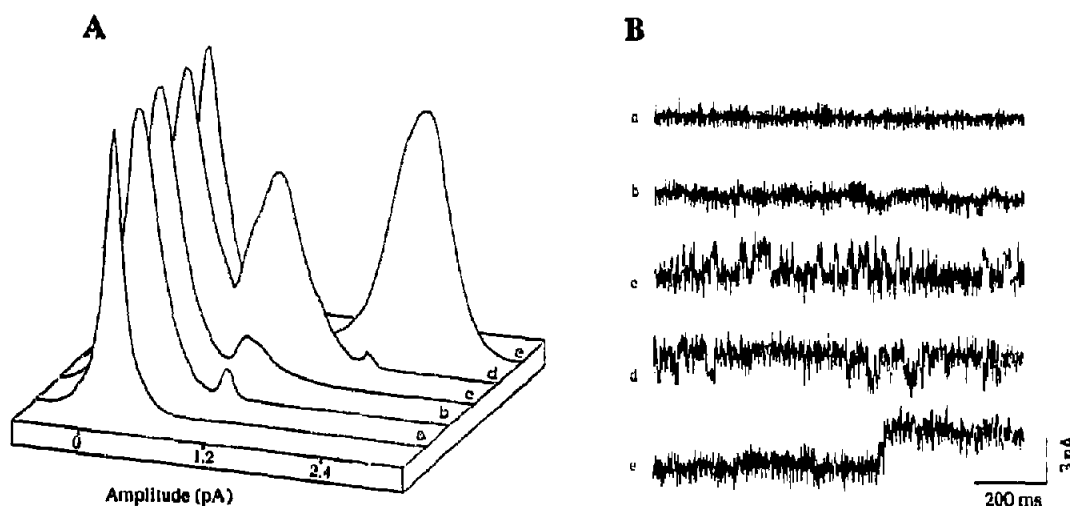


Fig. 3. (A) Amplitude histograms of channel currents activated by acetylcholine. Each maximum likelihood amplitude histogram was obtained from a segment of data containing 20,000 points by using digital signal processing techniques. For clarity, the peak of the histogram, representing the baseline current, was normalized to 1, rather than the area under the curve, and then 5 histograms so constructed from the same patch at a regular interval are exhibited sequentially. The first histogram (a), obtained immediately after the application of acetylcholine, shows no current peaks apart from the baseline. Shortly thereafter, the width of the baseline peak broadens (b) owing to the appearance of small channels such as those shown in Fig. 2. In addition, a small but distinct peak appears at 1.25 pA. The probability of channel currents being at this level increases rapidly (c and d). Finally, the amplitude of channel currents become predominantly 2.5 pA (e). (B). Sample traces, 1,000-point record each, are selected from the records from which the amplitude histogram curves are obtained and displayed on the left hand column, labelled a–e.

state. Fig. 4 shows selected segments of the channel events that occurred after those illustrated in Fig. 3. The steady current level, instead of being at the baseline, was shifted upwards from it, indicating that the channel remained open. From this level, the current level dropped back intermittently to the baseline or jumped to a higher level. Although the records illustrated are from one patch, the characteristics of channels in the 20 patches we have analyzed broadly conform with the behaviour of this channel.

4. DISCUSSION

The m3 sub-type of muscarinic acetylcholine receptors is normally linked to phosphatidylinositol metabolism [2]. It is suggested that stimulation of the receptor by acetylcholine activates phospholipase C, which releases IP_3 , which in turn mobilises Ca^{2+} from the intracellular stores culminating in the activation of K^+ channels [3,5]. The currents we observed are carried by potassium ions (Fig. 1B) and are mediated by G-proteins sensitive to pertussis toxin (Fig. 1Ad). We note here that the calcium-dependent currents associated with m1 and m3 sub-types produced in A9-L cells were insensitive to pertussis toxin [5]. It is not unusual for a receptor to couple with different G-proteins when it is produced in a heterologous expression system [2]. The presence of G-proteins in Sf9 cells has been demonstrated previously by the coupling of turkey β_2 -adrenergic receptor with endogenous insect G-proteins [13]. Moreover, anti-

bodies raised against mammalian G-proteins cross-react with G-proteins of Sf9 cells, implying that they are structurally similar (H. Reiländer, unpublished observation).

In stark contrast to ligand-gated channels, the characteristics of single channel currents we describe here are not invariant with time but change rapidly. The transition probability of being in one of the open states progressively increases as do the number of conductance states and their levels. Starting from the appearance of small and brief channel currents of about 0.3 pA in amplitude, the amplitude first doubles to 0.6 pA and then to 1.2 pA. With time, the current level steps to 2.5 pA, to 5 pA and occasionally to 7–8 pA and then back to the baseline. These stepwise increases in the amplitude of channel currents are reminiscent of the behaviour of single S channel currents in *Aplysia* [14], potassium channels in cultured hippocampal neurons induced by arachidonic acid [15], voltage-activated calcium channels inserted in lipid bilayers [16], and K^+ -selective channels in the kidney of *Amphiuma* [17].

Of the several possible explanations for the variable single channel conductance of the muscarinic acetylcholine-mediated channels, we favour the following. There are a number of small conducting units each of which constitutes an elementary conducting pore for potassium ions. Initially one, and subsequently two and four, of these pores become elastically coupled so that they predominantly open and close synchronously. With time, a further group of four pores becomes func-

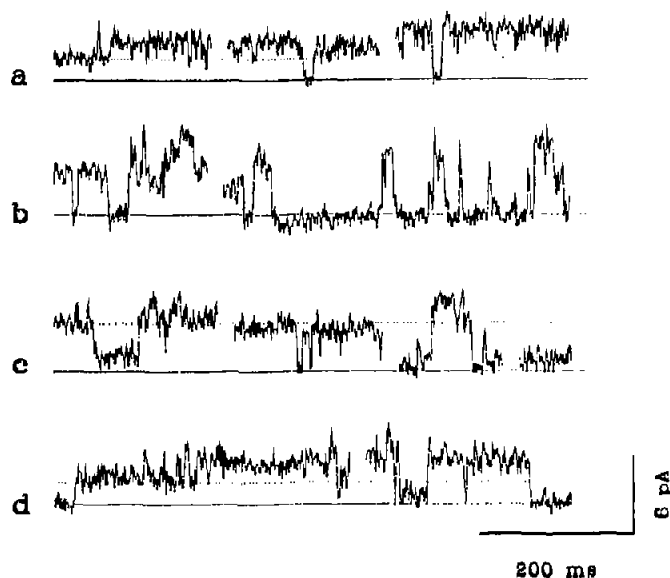


Fig. 4. Examples of outward currents in a cell-attached patch minutes after the application of acetylcholine. The selected segments of the record were obtained from the same patch as in Fig. 3. The records shown are obtained 1–3 min after the records used to construct the amplitude histogram d in the previous figure. The current level began to jump to 5 pA level, and then to 7–8 pA level. Frequently, the open channel current level returned to the baseline level, or channel current opened from the baseline to 5 pA level, in one digitizing interval of 100 μ s.

tionally coupled with the original four, thus causing the current level to fluctuate from the closed state to the 1.2 and 2.4 pA levels. This process of forming a large cluster of conducting pores continues so that currents as large as 7–8 pA can occur. One of the salient features of such an aggregate is that the conducting pores become partially coupled. Even from the largest conducting levels, all the channels often close instantaneously or in two or three steps within a short interval. Similarly, from the baseline level, the current can jump to the 5 pA or to the 7–8 pA level in one digital interval of 100 μ s. If each of the 16 elementary pores were to open or close independently of each other, the probability of all opening or closing simultaneously would have been low [18].

Whether or not the interpretation we propose here reflects the physical reality remains to be investigated.

Acknowledgements: Throughout the course of this study, Mrs. Somaja Louis provided excellent technical assistance, for which we are grateful. We also acknowledge the support and encouragement of W. Armarego, N. Dixon and H. Michel. This study was in part supported by grants from the National Health and Medical Research Council of Australia and the Ramaciotti Foundations.

REFERENCES

- [1] Stroud, R.M. and Finer-Moore, J. (1985) *Annu. Rev. Cell. Biol.* 1, 317–351.
- [2] Hulme, E.C., Birdsall, N.J.M. and Buckley, N.J. (1990) *Annu. Rev. Pharmacol. Toxicol.* 30, 633–673.
- [3] Neher, E., Marty, A., Fukuda, K., Kubo, T. and Numa, S. (1988) *FEBS Lett.* 240, 88–94.
- [4] Fukuda, K., Higashida, H., Kubo, T., Maeda, A., Akiba, I., Bujo, H., Mishina, M. and Numa, S. (1988) *Nature* 335, 355–358.
- [5] Jones, S.V.P., Barker, J.L., Goodman, M.B. and Brann, M.R. (1990) *J. Physiol.* 421, 499–519.
- [6] Klaiber, K., Williams, N., Roberts, T.M., Papazian, D. M., Jan, L.Y. and Miller, C. (1990) *Neuron* 5, 221–226.
- [7] Kartner, N., Hanrahan, J.W., Jensen, T.J., Nalsmith, A. L., Sun, S., Ackerley, C.A., Reyes, E.F., Tsui, L.-C., Rommens, J. M., Bear, C.E. and Riordan, J.R. (1991) *Cell* 64, 681–691.
- [8] Vasudevan, S., Reiländer, H., Maul, G. and Michel, H. (1991) *FEBS Lett.* 283, 52–56.
- [9] Chung, S.H., Moore, J.B., Xia, L., Premkumar, L.S. and Gage, P.W. (1990) *Phil. Trans. R. Soc. Lond. B* 329, 265–285.
- [10] Chung, S.H., Krishnamurthy, V. and Moore, J.B. (1991) *Phil. Trans. R. Soc. Lond. B* 334, 357–384.
- [11] Kitts, P.A., Ayres, M.D. and Porse, R.D. (1990) *Nucleic Acids Res.* 18, 5667–5672.
- [12] Summers, M.D. and Smith, G.E. (1987) *A Manual of Methods for Baculovirus Vectors and Insect Cell Culture Procedures*, Texas Experimental Station Bulletin 1555, Texas A&M College Station.
- [13] Parker, E.M. and Ross, E.M. (1991) *J. Biol. Chem.* 266, 9987–9996.
- [14] Piomelli, D., Volterra, A., Dale, N., Siegelbaum, S.A., Kandel, E.R., Schwartz, J.H. and Belardetti, F. (1987) *Nature* 328, 38–43.
- [15] Premkumar, L.S., Gage, P.W. and Chung, S.H. (1990) *Proc. R. Soc. Lond. B* 242, 17–22.
- [16] Glossmann, H. and Striessnig, J. (1988) *ISI Atlas of Science Pharmacology* 2, 202–210.
- [17] Hunter, M. and Giebisch, G. (1987) *Nature* 327, 522–524.
- [18] Krouse, M.E., Schneider, G.T. and Gage, P.W. (1986) *Nature* 319, 58–60.